Mat. Res. Soc. Symp. Proc. Vol. 746 © 2003 Materials Research Society Q4.4

Inert Gas Condensation of Iron and Iron-Oxide Nanoparticles

C. Baker,[1] S. Ismat Shah,[1,3,4] S.K. Hasanain,[2] B. Ali,[2] L. Shah,[2]
G. Li,[3] T. Ekiert,[3] and K.M. Unruh[3]

(1) Department of Materials Science and Engineering, University of Delaware, Newark, DE
(2) Department of Physics, Quaid-i-Azam University, Islamabad, Pakistan
(3) Department of Physics and Astronomy, University of Delaware, Newark, DE
(4) Fraunhofer Center for Manufacturing and Advanced Materials, Newark, DE

Abstract

An inert gas condensation technique has been used to prepare nanometer-sized particles of metallic iron by evaporation and agglomeration in a flowing inert gas stream. The resulting Fe nanoparticles were protected from complete oxidation either by the formation of a thin Fe-oxide surface passivation layer or by immersion in an oil bath. X-ray diffraction and transmission electron microscopy measurements indicated that the nanoparticles were typically between 10 and 20 nm in size, that the thickness of the Fe-oxide surface passivation layer was between 3 and 4 nm, and that the oil immersed samples exhibited a significant smaller volume fraction of Fe-oxides than did the surface passivated samples. Room temperature magnetization measurements were also carried out and the coercivity and saturation magnetization of the surface passivated and oil immersed samples determined. Although the coercivities and saturation magnetization values of both samples were very similar, the Fe/Fe-oxide samples exhibited a single component hysteresis loop while the Fe/oil samples exhibited a two component loop.

Introduction

Nanometer-sized Fe particles are pyrophoric and therefore must be protected from complete oxidation if they are to be exposed to atmospheric oxygen. The most common passivation procedure has been to form an Fe-oxide surface layer by slowly exposing the as-prepare nanoparticles to an oxygen containing environment.[1] Because the Fe-oxides are either antiferromagnetic (FeO, α-Fe_2O_3) or ferrimagnetic (γ-Fe_2O_3, Fe_3O_4),[2] however, the physical and chemical properties of these Fe/Fe-oxide nanoparticles reflect not only the properties of the Fe core but the properties of the passivation layer as well. For example, the hysteresis loops of these nanoparticles have often been observed to be shifted with respect to zero applied field when field cooled through the Néel temperature of the surface oxide due to an exchange coupling between the ferromagnetic core and the antiferromagnetic (or ferrimagnetic) surface oxide.[3]

Greater insight into the effects of finite size on the magnetic properties of small Fe particles, without the added complication of a core/shell exchange coupling, could be obtained by the study of particles passivated by a non-magnetic surface layer. Several schemes for achieving this have been reported in the literature including, for example, various chemical and physical methods for producing C, SiO_2, and Au coatings.[4-6] An alternative approach involves immersing the Fe nanoparticles into an oil prior to their exposure to air. This procedure does not result in the formation of a passivation layer *per se*, but does allow the Fe/oil mixture to be handled in

ambient air without significant oxidation. This approach not only has the advantage of simplicity (no subsequent processing steps other than immersion are required) but also results in minimal structural distortion of the nanoparticle surface.

The primary motivation for this work was to compare the structural and magnetic properties of two sets of Fe nanoparticles that differed only in the manner in which they were protected from oxidation. By comparing the magnetic properties of nanometer-sized Fe particles passivated with an Fe-oxide to those without a surface oxide (or at least a minimal amount of oxide) our goal was to gain a better understanding of the conditions required for the study of homogeneous, ferromagnetic Fe nanoparticles.

Experimental

All of the Fe nanoparticles studied in this work were prepared by an inert gas condensation (ICG) technique.[7] The procedure consisted of continuously feeding a high purity Fe wire toward a resistively heated Al_2O_3 coated W boat where it melted and evaporated. The resulting Fe vapor was entrained and cooled in a flowing stream of He gas where individual Fe atoms coalesced into small particles. These particles were deposited on a filter from which they were occasionally dislodged and collected in a removable container mounted to the bottom of the vacuum chamber. Fe/Fe-oxide nanoparticles were prepared by slowly exposing the collected Fe nanoparticles to a reduced pressure of atmospheric oxygen. Fe/oil samples were prepared by filling the collection container with vacuum pump oil and allowing the as-prepared Fe nanoparticles to settle into the oil as they were collected. In the latter instance, the oil immersed nanoparticles were subsequently filtered of excess oil to leave a thick Fe/oil residue.

The structure of both the Fe/Fe-oxide and Fe/oil samples was studied by x-ray diffraction (XRD) and transmission electron microscopy (TEM). In the former case, diffraction patterns were fit to a sum of two asymmetric Pearson VII functions representing the Cu $K_{\alpha 1}$ and Cu $K_{\alpha 2}$ components of the incident radiation. The resulting angular positions were used to obtain a best fit estimate of the lattice parameter while the width of the Fe (110) diffraction peak was used, in conjunction with the Scherrer formula, to estimate the mean particle size (after subtracting the measured natural line width in quadrature). Transmission electron microscopy samples were prepared by suspending a small quantity of the Fe nanoparticles in a volatile solvent, placing a small droplet onto a TEM grid, and allowing the solvent to evaporate. Both low magnification images and high magnification lattice images were obtained.

Magnetic properties measurements were carried out on disk shaped samples 4 mm in diameter and approximately 0.5 mm in thickness. A vibrating sample magnetometer (VSM) was used to measure the sample magnetization as a function of the applied field. The maximum applied field was 11 kOe and the law of approach to saturation was used to extrapolate the high field magnetization to its saturation value.[8]

The mass of the Fe nanoparticles in the Fe/oil samples was estimated based on the results of a series of XRD measurements on Fe/oil samples prepared from known amounts of (bulk) Fe powder mixed with the same oil used to protect the ICG prepared Fe samples. Fits to these data allowed a plot of the ratio of the Fe (110) peak area to the sum of the areas of the Fe (110) peak and the broad low angle oil scattering peak (see Fig. 1) as a function of the corresponding mass ratio to be constructed. A linear fit to these data (constrained to contain the origin) determined the proportionality constant between the peak areas and the mass ratios. This proportionality

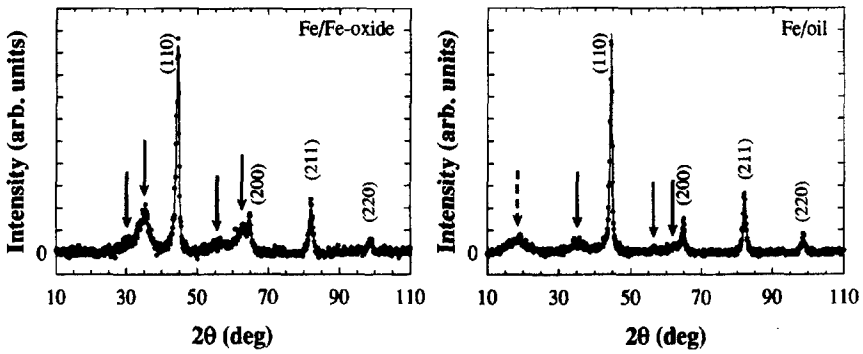

Figure 1: XRD patterns of Fe/Fe-oxide (left) and Fe/oil (right) samples. The solid lines are best fits to the data and the Miller indices of the metallic Fe phase have been indicated. The scattering peaks indicated by solid arrows probably correspond to γ-Fe_2O_3 as discussed in the text and the broad scattering peak indicated by a broken arrow in the Fe/oil sample arises from the oil.

constant was then used, in conjunction with the known total sample mass, to estimate the actual mass of the Fe nanoparticles in the Fe/oil samples.

Results and Discussion

Figure 1 shows typical XRD scattering patterns of Fe/Fe-oxide and Fe/oil samples, as well as the corresponding fits to the data. In both case the most intense scattering peaks arise from metallic Fe (indicated by their Miller indices) while the less intense peaks (indicated by solid arrows) probably arise from cubic γ-Fe_2O_3 although the cubic spinel Fe_3O_4 has a similar lattice parameter. The broad scattering peak centered at about 18 degrees (indicated by the broken arrow) in the Fe/oil sample arises from the oil used to protect the Fe nanoparticles. The best fit Fe lattice parameters of these two samples were $a=0.28707(3)$ *nm* and $a=0.28682(3)$ *nm*, respectively, for the Fe/Fe-oxide and Fe/oil samples; both of these values are slightly larger than the reported lattice parameter of bulk Fe ($a=0.28664$ *nm*) and may reflect some degree of oxygen incorporation into the Fe core.[9] Likewise, the effective lattice parameter of the γ-Fe_2O_3 phase was determined to be $a=0.835(4)$ *nm* and $a=0.834(4)$ *nm*, consistent with the previously reported value of $a=0.8346$ *nm* (the lattice parameter of Fe_3O_4 is $a=0.8396$ *nm*).[10] The corresponding Fe diameters of the Fe particle cores were $D=10.8(3)$ *nm* and $D=16.2$ *nm*. Based on a comparison of the area of the Fe (110) scattering peak to that of the most intense γ-Fe_2O_3 peak, the Fe/oil sample contains between 4 and 5 times less Fe-oxide than does the Fe/Fe-oxide sample.

Figure 2 shows a high magnification TEM lattice image taken from the Fe/Fe-oxide sample as well as a lower magnification image taken from an Fe/oil sample (higher magnification images were not taken because of the potential for contaminating the TEM sample space). For the Fe/Fe-oxide sample, it can be seen that the oxide layer surrounding the Fe is approximately 3 – 4 nm thick, and is crystalline in nature. The mean particle sizes estimated from the TEM images were in reasonable agreement with the corresponding values obtained from the Scherrer analysis of the XRD peak widths.

Figure 3 shows the room temperature hysteresis loops for the Fe/Fe-oxide and Fe/oil samples. The hysteresis loop of the Fe/Fe-oxide sample is characteristic of a single magnetic phase and exhibits a coercivity of $H_c=529$ *Oe* while the Fe/oil loop clearly exhibits two magnetic

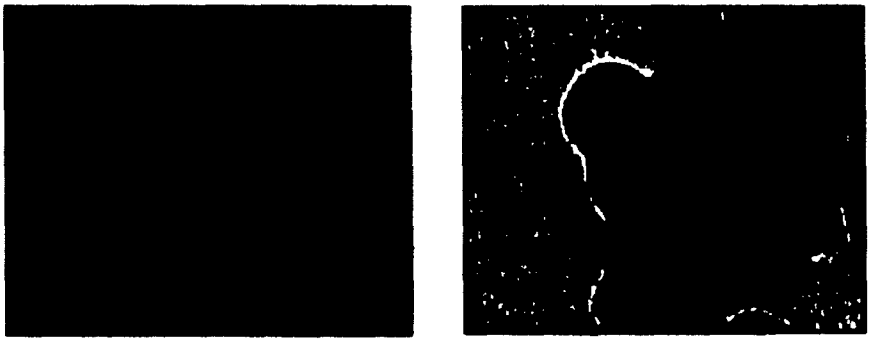

Figure 2: High resolution lattice image of Fe/Fe-oxide particle (left) and a low resolution image of Fe/oil coated particles. The particles shown in these images are not representative of average sized particles. Note the presence of the crystalline passivation layer surrounding the Fe core in the Fe/Fe-oxide image.

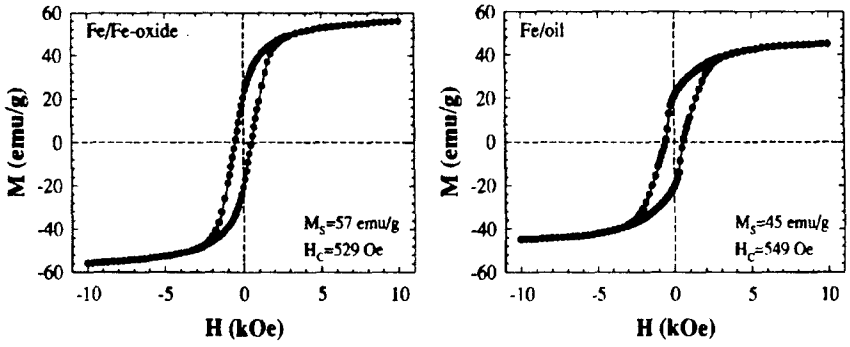

Figure 3: Room temperature hysteresis loops of Fe/Fe-oxide (left) and Fe/oil (right) samples. The saturation magnetization was determined based on an H^{-2} extrapolation of the measured high field magnetization using the total measured sample mass in the case of the Fe/Fe-oxide sample and the corrected sample mass as described in the text in the case of the Fe/oil sample.

components and a slightly larger coercivity of H_c=*549 Oe*. The saturation magnetization of both samples was estimated using the law of approach to saturation taking the first term in the field dependent magnetization to be proportional to H^{-2}. Based on the total particle mass, this procedure yielded a saturation magnetization of M_s=*57 emu/g* for the Fe/Fe-oxide sample and M_s=*45 emu/g* for the Fe/oil sample (after correcting the total sample mass for the oil contribution as described above). Given the uncertainties in correcting for the oil mass in the Fe/oil samples, the difference between the saturation magnetization values of the Fe/Fe-oxide and Fe/oil samples is probably not significant. A more detailed analysis of the magnetization would require additional information as to the amount, density, and specific magnetizations of the individual Fe-oxide and Fe phases.

The Fe/oil samples contain less Fe-oxide per particle and one might have expected the magnetic properties of these particles to be less reflective of a two phase system (i.e. an Fe-oxide surface layer and an Fe core) and more reflective of nanometer-sized ferromagnetic Fe. Although the magnetic data shown in Fig. 3b provides some support for this expectation in the form of a

two component hysteresis loop, the coercivity and saturation magnetization values indicate a similar magnetic structure. In particular, the fact that the observed coercivity is significantly larger than the value $H_c \approx 0.64 K_1/M_s \approx 177$ Oe predicted by the simple Stoner-Wohlfarth magnetization reversal model for a collection of randomly oriented single domain particles, assuming that the magnetocrystalline anisotropy and saturation magnetization for a nanometer-sized Fe particle assume their bulk values of $K_1 \approx 6 \times 10^4$ ergs/g and $M_s \approx 217$ emu/g,[11] suggests that both sets of samples are exchange coupled. Further evidence for an exchange coupled structure comes from an estimate of the effective magnetic anisotropy based on the law of approach to saturation. By fitting high field plots of $M_s(H)$ vs H^{-2}, or equivalently plots of χ vs H^{-3}, very similar values of $K_{eff}(cubic) \approx 2.3 \times 10^5$ erg/g or $K_{eff}(unixial) \approx 1.2 \times 10^5$ erg/g were obtained for the Fe/Fe-oxide and Fe/oil samples based on the assumption of either a cubic or a uniaxial anisotropy. Both values are significantly larger than the (cubic) anisotropy of bulk Fe.

Summary and Conclusion

We have developed a process in which Fe nanoparticles are synthesized by an IGC technique and protected from complete oxidation either by the formation of an Fe-oxide surface layer or by immersion in an oil. The magnetic behavior of the Fe/Fe-oxide and Fe/oil nanoparticles prepared in this way were then compared. Hysteresis loop measurements indicate that the presence of the Fe-oxide surface layer results in an exchange coupling between the surface moments and the moments of the entire Fe core in both samples, despite the significantly smaller amount of Fe-oxide present in the Fe/oil samples.

Acknowledgements

We are pleased to acknowledge Dr. C. Ni for has assistance with the TEM measurements. The work of SIS has been supported of the National Science Foundation through grant no. INT-0138151 and the work of KMU has been supported by AFRL DARPA METAMATERIALS contract no. F33615-01-2-2166.

References

1. See e.g. R.C. O'Handley, *Modern Magnetic Materials: Principles and Applications*, (John Wiley & Sons, Inc., New York, 2000).
2. See e.g. C.N.R. Rao and G.V. Rao, in *Transition Metal Oxides: Crystal Structure, Phase Transitions and Related Aspects* (NSRDS-NBS 49, 1974).
3. See e.g. W.H. Meiklejohn and C.P. Bean, *New Magnetic Anisotropy*, Phys. Rev. **105**, 904 (1957); J.F. Löffler, J.P. Meier, B. Doudin, J-P. Ansermet, and W. Wagner, *Random and Exchange Anisotropy in Consolidated Nanostructured Fe and Ni: Role of Grain Size and Trace Oxides on the Magnetic Properties*, Phys. Rev. B **57**(5), 2915 (1998); C. Prados, M. Multigner, A. Hernando, J.C. Sánchez, A. Fernández, C.F. Conde, and A. Conde, *Dependence of Exchange Anisotropy and Coercivity on the Fe-Oxide Structure in Oxygen-Passivated Fe Nanoparticles*, J. Appl. Phys. **85**(8), 6118 (1999). Two recent reviews on exchange coupled systems which contain many references can be found in J. Nogues and I.K. Schuller, *Exchange Bias*, J. Magn. Magn. Mater. **192**, 203 (1998) and A.E. Berkowitz and K. Takano, *Exchange Anisotropy – A Review*, J. Magn. Magn. Mater. **200**, 552 (1999).

4. S. Linderoth, L. Balcells, A. Laborta, J. Tajeda, P.V. Hendriksen, and S.A. Sethi, *Magnetization and Mössbauer studies of Ultrafine Fe-C particles*, J. Magn. Magn. Mater. **124**, 269 (1993).
5. E.E. Carpenter, *Iron Nanoparticles as Potential Magnetic Carriers*, J. Magn. Mag. Mater. **225**(1-2), 17 (2001).
6. T. Ibusuki, S. Kojima, O. Kitakami, and Y. Shimada, *Magnetic Anisotropy and Behaviors of Fe Nanoparticles*, IEEE Trans. Magn. **37**(4), 2223 (2001).
7. C.G. Granqvist and R.A. Buhrman, *Ultrafine Metal Particles*, -J. Appl. Phys. **47**(5), 2200 (1976).
8. S. Chikazumi, *Physics of Ferromagnetism*, (Clarendon Press, Oxford, 1997).
9. *Pearson's Handbook of Crystallographic Data for Intermetallic Phases*, edited by P. Villars and L.D. Calvert (American Society for Metals, Metals Park, Ohio, 1989).
10. T. Belin, N. Guigue-Millot, T. Caillot, D. Aymes, and J.C. Niepce, *Influence of Grain Size, Oxygen Stoichiometry, and Synthesis Conditions on the γ-Fe_2O_3 Vacancies and Lattice Parameters*, J. Solid State Chem. **163**, 459 (2002).
11. 14. E.C. Stoner and E.P. Wohlfarth, *A Mechanism of Magnetic Hysteresis in Heterogeneous Alloys*. Phil. Trans. Roy. Soc. London A **240**, 599 (1948).